



Published in final edited form as:

Circ Heart Fail. 2015 March ; 8(2): 352–361. doi:10.1161/CIRCHEARTFAILURE.114.001893.

Tumor Necrosis Factor: A Mechanistic Link between Angiotensin-II-Induced Cardiac Inflammation and Fibrosis

Clemens Duerrschmid, MS¹, JoAnn Trial, PhD¹, Yanlin Wang, MD, PhD², Mark L. Entman, MD¹, and Sandra B. Haudek, MS, PhD¹

¹Department of Medicine, Division of Cardiovascular Sciences, Baylor College of Medicine, Houston, TX

²Department of Medicine, Division of Nephrology, Baylor College of Medicine, Houston, TX

Abstract

Background—Continuous angiotensin-II (Ang-II) infusion induced the uptake of monocytic fibroblast precursors that initiated the development of cardiac fibrosis; these cells and concurrent fibrosis were absent in mice lacking tumor necrosis factor-alpha receptor 1 (TNFR1). We now investigated their cellular origin and temporal uptake, and the involvement of TNFR1 in monocyte-to-fibroblast differentiation.

Methods and Results—Within a day, Ang-II induced a pro-inflammatory environment characterized by production of inflammatory chemokines, cytokines, and T_H1-interleukins and uptake of bone marrow-derived M1-cells. After a week, the cardiac environment changed to profibrotic with growth-factor and T_H2-interleukin synthesis, uptake of bone marrow-derived M2-cells, and presence of M2-related fibroblasts. TNFR1 signaling was not necessary for early M1 uptake, but its absence diminished the amount of M2-cells. TNFR1-KO hearts also showed reduced levels of cytokine expression, but not of T_H-related lymphokines. Reconstitution of wild-type bone marrow into TNFR1-KO mice was sufficient to restore M2 uptake, upregulation of pro-inflammatory and pro-fibrotic genes, and development of fibrosis in response to Ang-II. We also developed an in vitro mouse monocyte-to-fibroblast-maturation assay that confirmed the essential role of TNFR1 in the sequential progression of monocyte activation and fibroblast formation.

Conclusions—Development of cardiac fibrosis in response to Ang-II was mediated by myeloid precursors and consisted of two stages. A primary M1 inflammatory response was followed by a subsequent M2 fibrotic response. While the first phase appeared to be independent of TNFR1 signaling, the later phase (and development of fibrosis) was abrogated by deletion of TNFR1.

Keywords

angiotensin; blood cell; collagen; inflammation; remodeling

Correspondence to Sandra B. Haudek One Baylor Plaza, BCM620 Houston, TX 77030 Phone: 1-713-798-3388 Fax: 1-713-796-0015 shaudek@bcm.edu.

Disclosures
None.

The development of cardiac interstitial fibrosis and concurrent development of ventricular remodeling in the absence of myocyte death is frequently associated with inflammatory reactions.^{1,2} Several inflammatory and fibrotic factors have been implicated in adverse cardiac remodeling, such as angiotensin-II (Ang-II) and tumor necrosis factor-alpha (TNF).³⁻⁵ Although the literature suggests synergistic actions of Ang-II and TNF,⁶⁻⁹ the cellular and molecular mechanisms for their interactions are still unclear.

In our previous work, we demonstrated that Ang-II exposure resulted in the immediate upregulation of monocyte chemoattractant protein-1 (MCP-1) in endothelial cells around small vessels, which attracted the influx of a distinct population of monocytic CD34⁺CD45⁺ fibroblast precursor cells into the myocardium.¹⁰ Once the transient MCP-1 signal decreased, the monocytic precursors disappeared as well. In mice deficient in MCP-1, Ang-II did not induce the appearance of this fibroblast population. Neither did these mice develop cardiac fibrosis in response to Ang-II stimulation, indicating that the development of interstitial fibrosis was initiated by the MCP-1-driven uptake of monocytic fibroblast precursors.¹⁰ We observed similar mechanisms in a chronic ischemia/reperfusion cardiomyopathy (I/RC) model (no infarct), in which upregulation of MCP-1 was also necessary for the uptake of bone marrow-derived fibroblast precursors and concurrent development of fibrosis.¹¹ Exposure of wild-type (WT) mice to Ang-II resulted in increased levels of myocardial TNF which were absent in Ang-II-challenged MCP1-KO mice.¹⁰ In subsequent studies, we found that mice with genetic deletion of TNF receptor 1 (TNFR1) were resistant to Ang-II-induced cardiac fibrosis, and presented lesser cardiac hypertrophy and better cardiac function than WT mice.¹² Mice deficient in TNF receptor 2 (TNFR2) were not different to WT in most parameters studied.¹²

Parallel to our in vivo work, we developed an in vitro assay of human monocyte-to-fibroblast maturation to replicate the in vivo events in respect to monocyte migration and differentiation.^{13,14} Utilizing this transendothelial migration assay, we recapitulated our in vivo observations: using mononuclear cells we demonstrated that endothelial transmigration in response to MCP-1 was necessary for monocytes to mature into fibroblasts.¹³ In addition, we showed that both Ang-II and TNF had to be present, as one or the other by itself did not increase the formation of fibroblasts from monocytes.¹²

In the current study, we defined the temporal sequence of the cellular and molecular events involved in Ang-II-mediated cardiac fibrosis. We found that early infiltrating bone marrow-derived monocytes polarized to classically activated M1-cells creating a pro-inflammatory environment, including the production of TNF. Within a few days, this response changed into a pro-fibrotic milieu: there was an uptake and/or differentiation of alternatively activated M2-cells that further developed into myeloid-derived fibroblasts, while M1 markers largely disappeared. In vitro, we newly developed a model using mouse monocytes from WT and TNFR1-KO mice and mouse endothelial cells to investigate the role of TNFR1 in mouse monocyte-to-fibroblast maturation.

Together, we found that signaling through TNFR1 was necessary for monocyte-to-fibroblast formation. Our data suggest that the production of TNF by pro-inflammatory cells supported

a TNFR1-mediated maturation process in pro-fibrotic M2-cells, and thus serves as a mechanistic link between Ang-II-induced cardiac inflammation and fibrosis.

Methods

Animals

Male and female C57BL/6-Tnfrsf1a^{tm1Imx/J} (TNFR1-KO) and C57BL/6J (WT) mice (8-10 weeks) were infused with 1.5 µg/kg/min Ang-II via subcutaneously implanted osmotic pumps; control animals received saline.^{10,12} Donor bone marrow was isolated from femur/tibias; recipient mice were irradiated with 100Gy and received ~10⁶ cells via tail-vein injection. Six-7 weeks later, animals received Ang-II. All mice were euthanized with 2% isoflurane followed by cervical dislocation. The investigations conformed to the *Guide for the Care and Use of Laboratory Animals* published by the NIH. All animals were treated in accordance with the guidelines of the Baylor College of Medicine Animal Care and Research Advisory Committee.

Flow cytometry

Hearts were excised and cells isolated by enzymatic digestion using 0.1 mg/ml LiberaseTH Research Grade.¹⁰⁻¹² Cells were incubated with calcein^{AM} (green-fluorescent after metabolization) together with directly-conjugated or biotin-conjugated external antibodies followed by PE- or PE/Cy5-conjugated secondary antibodies. In separate setups, cells were externally stained, permeabilized, then incubated with internal antibodies. FITC/PE/Cy-5 fluorescence intensities were measured on an EpicsXL-MCL or a CellLabQuantaSC with companion softwares (gating strategies are shown in Suppl.Fig.1A-B using FlowJo.X 10.0.7).

Tissue staining

Hearts were arrested in diastole, perfusion-fixed in Zinc-Tris buffer, and paraffin embedded.¹⁰⁻¹² (1) Rehydrated, permeabilized sections close to the mid-papillary level were stained with antibodies. Slides were mounted using FluoroshieldTM with DAPI and analyzed on an Olympus AX70 upright microscope. Monochrome images for each fluorescence channel were acquired using QCapturePro.6.0; composite images were created using Image.J (v1.46r, NIH). (2) Rehydrated sections were stained in 0.05% picosirius red and mounted in CytosealTMXYL. Bright-field images were captured on an Olympus.CKX41 inverted microscope using QCapturePro.5.0. Quantitative analysis of collagen-stained areas was calculated using ImageProPlus.5.1 to obtain percentages of the total myocardial area.

Quantitative PCR

RNA was isolated using Trizol-reagent; cDNA was synthesized using Verso Reverse Transcription. 1:10 dilutions of cDNA were run on a CX1000 TouchTM Thermal Cycler with a CFX96TM Real-Time System using SSOAdvancedTMSYBR® green mastermix (BioRad). All primers were validated according to MIQE guidelines (Suppl.Table 1).¹⁵ Relative gene expression compared to control was calculated using the Cq method.

Mouse transendothelial migration assay

Similar to reported protocols,^{11,12,14} mouse cardiac endothelial cells (MCEC, Cedarline) were seeded at 4×10^4 cells/insert. Mouse monocytes (25×10^4 ; isolated from untreated mouse spleen using EasySep™ Mouse Monocyte Enrichment) were added together with either saline or both Ang-II (1 ng/ml) and TNF (10 ng/ml) to the top well. Mouse MCP-1 (650 ng/ml) was added to the bottom well. After 4 days, adherent cells in the bottom well were stained with Giemsa and manually counted (see^{12,14} for detailed cell identification); each setup was measured in triplicate. In separate setups, migrated cells were allowed to adhere on coverslips for immunostaining.¹⁴

Statistical analysis

Kolmogorov-Smirnov tests were used to evaluate normal distribution, Bartlett's tests to evaluate differences among Standard Deviations. Unpaired two-tailed Student's t-tests (or Mann-Whitney if nonparametric) were used to compare differences between 2 groups. One-way ANOVA (or Kruskal-Wallis if nonparametric) were used to compare differences between >2 groups; Tukey-Kramer post-hoc testing (or Dunn's if nonparametric) were performed when appropriate. A P-value <0.05 was considered statistically significant (GraphPad InStat 3.06). Data in text and figures are expressed as mean \pm SEM, except for box plots.

Results

Infusion of Ang-II to WT mice induced the immediate presence of M1-cells and delayed presence of M2-cells

To study the temporal profile of Ang-II-induced uptake of infiltrating cells, we performed immunostaining on WT hearts. As shown in Fig.1A, at 1 day we found many CD86⁺ M1-cells, but only few at 7 days; these cells were negative for pro-collagen-type-I. By contrast, at 1 day we found few M2-cells, but many M2-cells after 7 days that were also positive for pro-collagen-type-I (CD301⁺, Fig.1B; CD206⁺, Fig.1C). We obtained similar results using inducible nitric oxide synthase (iNOS) and arginase as additional M1/M2 markers (Suppl.Fig.2). Next, we isolated cells from WT hearts and performed cytometry. We observed an early appearance of hematopoietic M1-cells (CD86⁺CD45⁺: $1.5 \pm 0.2\%$, Fig. 1D1) that decreased to $0.8 \pm 0.1\%$ after 7 days. We obtained similar results using CD16/32 as an M1 marker (Suppl.Fig.3A1/2). By contrast, at early times, we detected only few M2-cells (CD301⁺CD45⁺: $0.1 \pm 0.1\%$, Fig.1E1; CD206⁺CD45⁺: $2.2 \pm 0.2\%$, Fig.1F1). However, these numbers increased by 7 days to $4.8 \pm 0.3\%$ and $5.0 \pm 0.5\%$, indicating a predominance of M2-cells after longer Ang-II infusion. Likewise, the number of CD301⁺ (Fig.1E2) and CD206⁺ (Fig.1F2) cells that also expressed collagen-type-I increased over time, as did M2-cells that were positive for α -smooth muscle actin (α SMA; Suppl.Fig.4). We obtained similar results using CD150 as an M2 marker (Suppl.Fig.3B1/2). Many M2-cells, but not M1-cells were also positive for the precursor marker CD34 (Suppl.Fig.5). Taken together, Ang-II induced an early uptake of pro-inflammatory M1-cells that decreased over the first week, while the number of anti-inflammatory M2-cells, that also expressed fibroblast markers, increased over the same time period.

Infusion of Ang-II to TNFR1-KO mice induced the immediate presence of M1-cells, but the delayed appearance of M2-cells was absent

We found that the amount of CD86⁺CD45⁺ M1-cells in TNFR1-KO hearts was not different compared to WT levels at both 3- and 7-day Ang-II infusion (1.4±0.2% and 0.7±0.1%; Fig. 1D1). However, the amounts of CD301⁺CD45⁺ (Fig. 1E1) and CD206⁺CD45⁺ (Fig. 1F1) M2-cells were lower at 7 days (0.8±0.4% and 1.9±0.2%) than the corresponding levels in WT mice. Similarly, the numbers of collagen-type-I positive CD301⁺ (Fig. 1E2) and CD206⁺ (Fig. 1F2) M2-cells were also lower in TNFR1-KO than in WT hearts. We obtained similar results using CD16/32 and CD150 as M1/M2 markers (Suppl.Fig.3A-B). These data indicated that TNFR1 signaling was not involved in the uptake of M1-cells, but lack of TNFR1 reduced the uptake and/or polarization of CD45⁺ monocytes into M2-cells in the Ang-II-challenged heart. Of note, the kinetics of Ang-II-induced cellular uptake in TNFR2-KO hearts did not differ from WT levels (Suppl.Fig.6), supporting our previous results that TNFR2 was not involved in the Ang-II-induced cardiac fibrosis.¹²

Infusion of Ang-II to WT mice induced the immediate increase of pro-inflammatory factors and the delayed increase of pro-fibrotic factors

We have previously described an upregulation of distinct inflammatory and fibrotic proteins in the WT heart after 7-day Ang-II infusion.^{10,12} We now extended these observations by evaluating expression levels at earlier time points (1 and 3 days) and including additional factors (IL-1 β , IFN- γ , IL-4, IL-13). We found that transcriptional activation of TNF was immediately upregulated and persisted until at least 7 days (Fig.2A). Other pro-inflammatory factors such as MCP-1, IL-1 β , IL-6, and IFN- γ were also highly upregulated early (Figs.2B-E), whereas anti-inflammatory and/or pro-fibrotic factors, such IL-4, IL-13, TGF β -1, and osteopontin were maximally increased after 7 days (Figs.2F-I).

Infusion of Ang-II to TNFR1-KO mice did not increase levels of M1- or M2- related factors, but increased T_H1- and T_H2- related factors

Similar to our earlier 7-day study,¹² in TNFR1-KO hearts we found reduced expression levels of genes associated with inflammation (TNF, MCP-1, IL-1 β , IL-6; Figs.2A-D) and fibrosis (TGF- β 1, osteopontin; Figs.2H-I) compared to WT levels. However, synthesis of T_H1 (IFN- γ) and T_H2 (IL-4, IL-13) products were unaffected by deletion of TNFR1 (Figs. 2E-G). These data indicated that TNFR1 signaling was necessary for cytokine, chemokine, and growth factor activation, but not for lymphokine production.

Ang-II-induced TNF production was associated with M1-cells, but not with M2-cells, while both expressed TNFR1

Production of TNF in the Ang-II-challenged WT heart was found to be co-located to CD45⁺ cells, specifically cells that were CD86⁺ (Figs.3A-B1: immunostaining; Figs.3A-B2: cytometry). TNF was not found in areas of little cellular infiltration. Notably, TNF production was not associated with cells expressing CD301 or CD206 (Figs.3C-D). Expression of TNFR1 in Ang-II-challenged WT hearts was positive on both M1 and M2 populations (Figs.3E-H) and was associated with high expression of CD45 (CD45^{high}; Suppl.Fig.7). The kinetics of transcriptional TNFR1 expression was similar to that of TNF

(Suppl.Fig.8). These findings suggest that TNF was primarily produced by infiltrating, pro-inflammatory cells, but that both M1-cells and M2-cells could respond to TNF via TNFR1.

Ang-II-induced fibroblast precursors were of bone marrow origin and their uptake depended on TNFR1 signaling

We found that chimeric TNFR1-KO mice with WT-bone marrow mounted a similar fibrotic response as WT mice:

1) As shown in Figs.4A1/2 (and Suppl.Fig.9), after 7 days, chimeric TNFR1-KO/WT mice developed cardiac fibrosis. Specifically, levels of collagen deposition in these hearts ($5.7\pm 0.6\%$) were comparable to those in WT hearts ($5.2\pm 1.0\%$) and significantly higher than in TNFR1-KO hearts ($2.0\pm 0.1\%$). 2) In chimeric TNFR1-KO/WT mice, mRNA expression levels of collagen-types -I and -III, TNF, IL-1 β , and TGF- β 1 (Fig.4B) were restored to WT levels and were significantly greater than in TNFR1-KO hearts. 3) In chimeric TNFR1-KO/WT mice, infiltrating cells - defined by their positive TNFR1 expression because of their WT bone marrow origin - were highly present in numbers equal to WT levels (Fig.4C, immunostaining; Suppl.Fig.10, quantification). Moreover, many of these cells were also positive for α SMA, indicating their commitment to a fibroblast lineage (Fig.4C). 4) We identified increased amounts of M2-cells (CD301⁺CD45⁺, CD206⁺CD45⁺) in the chimeric TNFR1-KO/WT heart (Figs.5AB1), as well as increased numbers of CD34⁺CD45⁺ precursors (Fig.5C1); all 3 populations were also positive for collagen-type-I expression (Figs.5A-C2). Taken together, these data confirm that infiltrating myeloid fibroblast precursor cells were of bone marrow origin and that TNFR1 was necessary for their uptake and maturation in the heart.

In vitro, mouse monocyte-to-fibroblast maturation depended on TNFR1 signaling

Previously, we have exclusively used human mononuclear cells and antibody-mediated inhibition/activation.^{12-14,16} In the current study, we developed an assay using cells from genetically altered mice. We isolated mouse monocytes from untreated WT and TNFR1-KO mice and subjected them to migration through mouse endothelial cells in response to MCP-1. After 4 days, we found significantly more fibroblasts in the Ang-II/TNF-stimulated WT cells than in the Ang-II/TNF-stimulated TNFR1-KO cells (Fig.6A); the amount of fibroblasts in Ang-II/TNF-stimulated TNFR1-KO cells was not different than in the unstimulated TNFR1-KO or unstimulated WT setups. Further, adherent WT cells after 4-6 days were spindle-shaped and expressed CD206 and CD301, together with pro-collagen-type-I (Figs.6B-C), indicating their M2-related fibroblast phenotype. These cells also expressed TNFR1 (Fig.6D). By contrast, adherent cells after 1 day were primarily round and positive for M1 markers CD86 and iNOS (Fig.6E), similar to our recent human in vitro reports.¹⁴ These in vitro data expand our previous observations indicating that TNFR1 signaling was necessary for the Ang-II-induced monocyte-to-fibroblast maturation.

Discussion

This report extends our studies into the mechanism by which chemokine induction results in the rapid onset of interstitial cardiac fibrosis. Our laboratory has focused on two murine

models of non-infarctive injury; an ischemic reperfusion cardiomyopathy (I/RC)¹⁷ and an Ang-II infusion protocol,¹⁰ both leading to cardiac hypertrophy, remodeling, and fibrosis. We found remarkably similar characteristics: 1) MCP-1 upregulation was prolonged (up to 1 week).^{10,17} 2) Myeloid fibroblast precursor cells appeared in the heart.^{10,11} 3) MCP-1 was required to attract this myeloid cell population, as these cells were absent in MCP-1-KO hearts.^{10,18} 4) Myeloid fibroblasts were distinct in morphology and proliferation activity and expressed CD34, CD45, and CCR2 (MCP-1 receptor),^{10,11,19} distinguishing them from tissue-resident cells; they were also positive for typical fibroblast markers (collagen-type-I, α SMA, DDR2).^{10-13,16} 5) By means of bone marrow transplantation experiments using either β -galactosidase-labeled cells (I/RC)¹¹ or cells lacking TNFR1 (Ang-II infusion; current study), we showed that this myeloid fibroblast population was of bone marrow origin, and its uptake required mechanisms involving TNFR1 signaling. 6) Cardiac fibrosis peaked within the first 2 weeks and persisted as long as the stimulus was administered,^{10,17} however, the fibroblast precursor population disappeared as soon as MCP-1 induction diminished (after 1 week). Therefore, MCP-1 activation and appearance of CD34⁺CD45⁺ precursor cells were required for triggering the development of cardiac fibrosis, but other mechanisms drove maintenance and progression. The authors want to emphasize that this unique, chemokine-dependent mechanism of myeloid fibroblast generation does not account for all of the mechanisms by which fibroblasts may be generated as part of growth and/or in response to pathological stimuli, as discussed below.

Chemokine-dependent fibrosis

Our study targets an acute inflammatory/fibrotic response modulated by chemokine, cytokine, and T-lymphocyte products that results in the formation of myeloid fibroblasts, and the cellular signaling associated with its generation. We and others have demonstrated a similar chemokine-dependent inflammatory response associated with obstructive and Ang-II-generated renal disease and pulmonary fibrosis.¹⁹⁻²² We have also studied the role of chronic cardiac inflammation and fibrosis associated with aging. We observed the presence of CD45⁺ myeloid fibroblasts persisting and increasing with time in the aging mouse heart; their presence was associated with persistent and increasing MCP-1 induction that may account, at least in part, for the ongoing presence of myeloid fibroblasts.²³ In these aging studies, we also described another distinct class of fibroblasts arising from CD44⁺CD45⁻ mesenchymal stem cells that differentiate normally into collagen-secreting cells, but failed to express α SMA in response to TGF β , which distinguished this cell population from the myeloid fibroblast population in the I/RC and Ang-II models.²⁴

Origin of myeloid fibroblasts

We previously reported the uptake of monocytic CD34⁺CD45⁺ fibroblast precursors in the Ang-II-exposed heart.^{10,12} We now expand these observations by performing bone marrow transplantation experiments for fibroblast lineage tracing. By irradiating TNFR1-KO mice and reconstituting their bone marrow with WT cells, we restored expression of TNFR1 in cells of the myeloid lineage. Using such chimeric TNFR1-KO/WT mice for Ang-II infusion, we found that, although TNFR1 was not present on resident cells, the presence of TNFR1 on bone marrow cells was sufficient to restore the development of Ang-II-induced cardiac fibrosis to the same extent as observed in WT hearts (Figs.4-5; Suppl.Figs.9-10). Since

many of the TNFR1⁺ cells in chimeric TNFR1-KO/WT mice were also positive for α SMA, we provide evidence that 1) fibroblast precursors were of bone marrow origin, and 2) TNFR1 signaling was involved in their uptake and/or maturation into myofibroblasts.

Myeloid fibroblasts may also derive from endogenous macrophages. Recent studies describe tissue-resident macrophages arising from yolk-sac progenitors: In the central nervous system, monocyte-derived macrophages were shown to express CD45^{high}, whereas microglia-derived resident macrophages were CD45^{low}.²⁵ In our study we found that most TNFR1⁺ cells in mouse heart after Ang-II infusion were CD45^{high} (Suppl.Fig.7), suggesting that these cells are of monocyte origin rather than tissue-resident. In the heart, in response to Ang-II, a resident macrophage population of embryonic origin was shown to expand by proliferation in addition to uptake of monocyte-derived macrophages, but this resident population did not express CCR2, nor was it responsive to MCP-1.²⁶ In our study, the presence of fibroblast precursors was MCP-1-dependent, again suggesting that these cells rather arise from monocytes. Another report also described a critical role for resident macrophages in the steady-state heart, however, when homeostasis was perturbed by myocardial infarction, macrophages mostly derived from blood monocytes.²⁷ Another study using the PDGF α receptor for fate specification suggested a precursor that has selective multipotentiality for various mesenchymal cells that may include fibroblasts.²⁸ The role of different mesenchymal subpopulations in cardiac, perhaps more chronic, fibrosis represents an ongoing interest of our group as well. We do not rule out a participation of such resident precursors; however, the role of this population in the chemokine-dependent inflammatory fibrosis described here is unlikely.

Uptake of myeloid fibroblasts

Within one day of Ang-II infusion we observed the uptake of M1-cells in the heart, concurrent with increased synthesis of MCP-1, TNF, distinctive cytokines and T_H1-related interleukins, altogether creating a pro-inflammatory environment (Figs.1-3; Suppl.Figs.2-3, 8). Later, at 7-day Ang-II infusion, the number of M1-cells declined, while M2-cells emerged; these cells were not associated with TNF, but with collagen, production (Figs.1, 3; Suppl.Figs.2-4, 8). We also observed simultaneous synthesis of distinct pro-fibrotic factors and T_H2-related interleukins (Fig.2). This sequential appearance of M1- and M2- related cells and products indicated that an initial, pro-inflammatory environment gradually transitioned into a later anti-inflammatory and profibrotic milieu.

At this point the authors cannot distinguish if the observed M2-cells polarized from M1-cells or were generated from a separate monocytic subpopulation (or both), and this may be difficult to test in vivo. Based on in vitro observations, in which we eliminate early migrating M1-cells from the assay and still found increased numbers of later migrating M2-cells,¹⁴ we hypothesize that in our model M2-cells mature from separate precursors instead of being generated by M1-to-M2-conversion. The existence of different precursor subpopulations may be supported by our observations that CD34 expression on cardiac fibroblast precursors (Suppl.Fig.5). CD34 has been regarded as a primitive cell marker, but has gained interest due to its involvement in asymmetric cell division of precursor cells,²⁹ and CD34 expression may be necessary for the ability of M2 to form a fibroblast. Since the

appearance of CD34⁺CD45⁺ cells correlated with the appearance of M2-cells, and M2-cells, but not M1-cells, expressed CD34, we can speculate that CD34 was necessary for M2-to-fibroblast formation, and/or only those M2-cells that expressed CD34 polarized into fibroblasts. Together with our observations that systolic blood pressure was also lower in Ang-II-infused TNFR1-KO mice,¹² the contribution of vascular remodeling to the cellular uptake of different precursors may also be a decisive factor in guiding the migration and/or maturation of these subpopulations. Further experiments to investigate these hypotheses are currently ongoing.

Role of TNFR1

This paper was designed to affirm the hypothesis of specific interactions of Ang-II and TNF and further pursue the mechanisms of that interaction. In mice with genetic deletion of TNFR1 we found little evidence for M2 generation in the Ang-II-exposed heart, whereas the amount of infiltrating M1-cells was not different than WT levels (Fig.1, Suppl.Fig.3A). The uninhibited influx of M1-cells in TNFR1-KO hearts indicated that the onset of inflammation was independent of TNFR1 signaling. However, signaling through TNFR1 played an important role in the transition to a fibrotic environment that favored fibroblast maturation and collagen deposition. Our initial studies demonstrated that MCP-1 deletion largely inhibited TNF induction and macrophage influx in response to Ang-II.¹⁰ It is thus likely that TNF was a principal agent in M1 mediation of the cellular progression of fibrosis. From our data, TNF should now be considered as an additional influence on inflammation resolution leading to fibrosis, rather than being a strictly pro-inflammatory mediator. Future studies should investigate whether M1 inflammation is reduced by an autocrine response to its own TNF product, thus allowing M2 precursors to respond to T_H2 mediators IL-4 and IL-13, or whether M2-to-fibroblast differentiation is directly aided by TNF, or both.

In vitro model of monocyte-to-fibroblast maturation

Parallel to our in vivo studies, we developed an in vitro assay that allowed a more careful examination of quantitative, qualitative, and temporal aspects of monocyte migration and polarization that are not directly addressable in vivo.^{13,14} In this assay we observed the maturation of human mononuclear cells into myeloid-derived fibroblasts after successful MCP-1-mediated migration through a human endothelial layer. We characterized the requirement of MCP-1-guided transendothelial migration, the inhibitory effects of serum amyloid P, the involvement of ROCK-1 signaling, and the requirement of IL-13 production for monocyte-to-fibroblast differentiation.^{10,13,16,23} Important for the current study, we demonstrated that neither Ang-II nor TNF alone was able to promote monocyte-to-fibroblast formation, but both agents had to be present at the same time.¹² We now developed a similar assay using mouse WT and TNFR1-KO monocytes and mouse endothelium. We were thus able to further characterize the temporal development of mouse fibroblast formation. Specifically, we show that also in vitro TNFR1 was necessary for Ang-II-stimulated monocyte-to-fibroblast generation (Fig.6). Moreover, we have established a novel assay protocol that allows us to use cells from any genetically manipulated mice to test for specific factors involved in monocyte-to-fibroblast formation, and future studies using cells from diverse mouse strains are warranted.

Conclusion

Ang-II-induced MCP-1 upregulation resulted in the sequential and timely regulated uptake of bone marrow cells and induction of pro-inflammatory and pro-fibrotic factors that drove the maturation of myeloid precursors into fibroblasts. Specifically (Fig.7), MCP-1 induced the uptake of monocytic precursors that polarized to cytokine-producing M1-cells that, together with T_H1-related factors, created a pro-inflammatory environment. At later times, infiltrating monocytes became M2-cells, which was influenced by concurrent production of T_H2-related proteins and generation of distinct pro-fibrotic factors. This pro-fibrotic milieu drove the maturation of an M2 subpopulation further to fibroblasts that produced and secreted collagen, leading to cardiac fibrosis and remodeling.

Importantly, our study suggests that TNF produced by M1-cells was necessary for mediating a TNFR1-dependent maturation of M2-cells into collagen-producing fibroblasts providing further evidence for an Ang-II/TNF synergy. A newly developed in vitro model of transendothelial migration of mouse WT and TNFR1-KO monocytes reproduced the signaling and temporal aspect of M2-to-fibroblast development. Thus, we provide evidence for a mechanistic link between Ang-II-induced inflammation and concurrent cardiac fibrosis.

Supplementary Material

Refer to Web version on PubMed Central for supplementary material.

Acknowledgments

We thank Naveeshini Chandran, Rohan Shah, Kathlene Boyle, Dorellyn Lee, and Jennifer Pocius for expert assistance.

Sources of Funding

This work was supported by the American Heart Association [10SDG4280031], Medallion Foundation, Hankamer Foundation, and NIH [R01DK95835, R01HL089792].

References

1. Nicoletti A, Michel JB. Cardiac fibrosis and inflammation: interaction with hemodynamic and hormonal factors. *Cardiovasc Res.* 1999; 41:532–543. [PubMed: 10435025]
2. Porter KE, Turner NA. Cardiac fibroblasts: at the heart of myocardial remodeling. *Pharmacol Ther.* 2009; 123:255–278. [PubMed: 19460403]
3. Gonzalez A, Lopez B, Querejeta R, Diez J. Regulation of myocardial fibrillar collagen by angiotensin-II. A role in hypertensive heart disease? *J Mol Cell Cardiol.* 2002; 34:1585–1593. [PubMed: 12505057]
4. Sciarretta S, Paneni F, Palano F, Chin D, Tocci G, Rubattu S, Volpe M. Role of the renin angiotensin-aldosterone system and inflammatory processes in the development and progression of diastolic dysfunction. *Clin Sci (Lond).* 2009; 116:467–477. [PubMed: 19200056]
5. Kleinbongard P, Heusch G, Schulz R. TNFalpha in atherosclerosis, myocardial ischemia/reperfusion and heart failure. *Pharmacol Ther.* 2010; 127:295–314. [PubMed: 20621692]
6. Kalra D, Sivasubramanian N, Mann DL. Angiotensin-II induces TNF biosynthesis in the adult mammalian heart through a protein kinase C-dependent pathway. *Circulation.* 2002; 105:2198–2205. [PubMed: 11994255]

7. Sriramula S, Haque M, Majid DS, Francis J. Involvement of TNF-alpha in angiotensin-II-mediated effects on salt appetite, hypertension, and cardiac hypertrophy. *Hypertension*. 2008; 51:1345–1351. [PubMed: 18391105]
8. Pellieux C, Montessuit C, Papageorgiou I, Lerch R. Angiotensin-II downregulates the fatty acid oxidation pathway in adult rat cardiomyocytes via release of TNF-alpha. *Cardiovasc Res*. 2009; 82:341–350. [PubMed: 19131364]
9. Wang Y, Li Y, Wu Y, Jia L, Wang J, Xie B, Hui M, Du J. TNF-alpha and IL-1beta Neutralization Ameliorates Angiotensin-II-Induced Cardiac Damage in Male Mice. *Endocrinology*. 2014; 155:2677–2687. [PubMed: 24877626]
10. Haudek SB, Cheng J, Du J, Wang Y, Hermosillo-Rodriguez J, Trial J, Taffet GE, Entman ML. Monocytic fibroblast precursors mediate fibrosis in angiotensin-II-induced cardiac hypertrophy. *J Mol Cell Cardiol*. 2010; 49:499–507. [PubMed: 20488188]
11. Haudek SB, Xia Y, Huebener P, Lee JM, Carlson S, Crawford JR, Pilling D, Gomer RH, Trial J, Frangogiannis NG, Entman ML. Bone marrow-derived fibroblast precursors mediate ischemic cardiomyopathy in mice. *Proc Natl Acad Sci U S A*. 2006; 103:18284–18289. [PubMed: 17114286]
12. Duerschmid C, Crawford JR, Reineke E, Taffet GE, Trial J, Entman ML, Haudek SB. TNF receptor 1 signaling is critically involved in mediating angiotensin-II-induced cardiac fibrosis. *J Mol Cell Cardiol*. 2013; 57C:59–67. [PubMed: 23337087]
13. Haudek SB, Trial J, Xia Y, Gupta D, Pilling D, Entman ML. Fc receptor engagement mediates differentiation of cardiac fibroblast precursor cells. *Proc Natl Acad Sci U S A*. 2008; 105:10179–10184. [PubMed: 18632582]
14. Trial J, Cieslik KA, Haudek SB, Duerschmid C, Entman ML. Th1/M1 conversion to th2/m2 responses in models of inflammation lacking cell death stimulates maturation of monocyte precursors to fibroblasts. *Front Immunol*. 2013; 4:287. [PubMed: 24065967]
15. Bustin SA, Benes V, Garson JA, Hellemans J, Huggett J, Kubista M, Mueller R, Nolan T, Pfaffl MW, Shipley GL, Vandesompele J, Wittwer CT. The MIQE guidelines: minimum information for publication of quantitative real-time PCR experiments. *Clin Chem*. 2009; 55:611–622. [PubMed: 19246619]
16. Haudek SB, Gupta D, Dewald O, Schwartz RJ, Wei L, Trial J, Entman ML. Rho kinase-1 mediates cardiac fibrosis by regulating fibroblast precursor cell differentiation. *Cardiovasc Res*. 2009; 83:511–518. [PubMed: 19406912]
17. Dewald O, Frangogiannis NG, Zoerlein M, Duerr GD, Klemm C, Knuefermann P, Taffet G, Michael LH, Crapo JD, Welz A, Entman ML. Development of murine ischemic cardiomyopathy is associated with a transient inflammatory reaction and depends on reactive oxygen species. *Proc Natl Acad Sci U S A*. 2003; 100:2700–2705. [PubMed: 12586861]
18. Frangogiannis NG, Dewald O, Xia Y, Ren G, Haudek S, Leucker T, Kraemer D, Taffet G, Rollins BJ, Entman ML. Critical role of monocyte chemoattractant protein-1/CC chemokine ligand 2 in the pathogenesis of ischemic cardiomyopathy. *Circulation*. 2007; 115:584–592. [PubMed: 17283277]
19. Xu J, Lin SC, Chen J, Miao Y, Taffet GE, Entman ML, Wang Y. CCR2 mediates the uptake of bone marrow-derived fibroblast precursors in angiotensin-II-induced cardiac fibrosis. *Am J Physiol Heart Circ Physiol*. 2011; 301:H538–H547. [PubMed: 21572015]
20. Xia Y, Jin X, Yan J, Entman ML, Wang Y. CXCR6 plays a critical role in angiotensin-II-induced renal injury and fibrosis. *Arterioscler Thromb Vasc Biol*. 2014; 34:1422–1428. [PubMed: 24855055]
21. Uchida M, Shiraishi H, Ohta S, Arima K, Taniguchi K, Suzuki S, Okamoto M, Ahlfeld SK, Ohshima K, Kato S, Toda S, Sagara H, Aizawa H, Hoshino T, Conway SJ, Hayashi S, Izuhara K. Periostin, a matricellular protein, plays a role in the induction of chemokines in pulmonary fibrosis. *Am J Respir Cell Mol Biol*. 2012; 46:677–686. [PubMed: 22246863]
22. Besnard AG, Struyf S, Guabiraba R, Fauconnier L, Rouxel N, Proost P, Uytendhoeve C, Van SJ, Couillin I, Ryffel B. CXCL6 antibody neutralization prevents lung inflammation and fibrosis in mice in the bleomycin model. *J Leukoc Biol*. 2013; 94:1317–1323. [PubMed: 23975892]

23. Cieslik KA, Taffet GE, Carlson S, Hermosillo J, Trial J, Entman ML. Immune-inflammatory dysregulation modulates the incidence of progressive fibrosis and diastolic stiffness in the aging heart. *J Mol Cell Cardiol.* 2011; 50:248–256. [PubMed: 20974150]
24. Cieslik KA, Trial J, Crawford JR, Taffet GE, Entman ML. Adverse fibrosis in the aging heart depends on signaling between myeloid and mesenchymal cells; role of inflammatory fibroblasts. *J Mol Cell Cardiol.* 2014; 70:56–63. [PubMed: 24184998]
25. Yamasaki R, Lu H, Butovsky O, Ohno N, Rietsch AM, Cialic R, Wu PM, Doykan CE, Lin J, Coteleur AC, Kidd G, Zorlu MM, Sun N, Hu W, Liu L, Lee JC, Taylor SE, Uehlein L, Dixon D, Gu J, Floruta CM, Zhu M, Charo IF, Weiner HL, Ransohoff RM. Differential roles of microglia and monocytes in the inflamed central nervous system. *J Exp Med.* 2014; 211:1533–1549. [PubMed: 25002752]
26. Epelman S, Lavine KJ, Beaudin AE, Sojka DK, Carrero JA, Calderon B, Brija T, Gautier EL, Ivanov S, Satpathy AT, Schilling JD, Schwendener R, Sergin I, Razani B, Forsberg EC, Yokoyama WM, Unanue ER, Colonna M, Randolph GJ, Mann DL. Embryonic and adult-derived resident cardiac macrophages are maintained through distinct mechanisms at steady-state and during inflammation. *Immunity.* 2014; 40:91–104. [PubMed: 24439267]
27. Heidt T, Courties G, Dutta P, Sager HB, Sebas M, Iwamoto Y, Sun Y, Da SN, Panizzi P, van der Lahn AM, Swirski FK, Weissleder R, Nahrendorf M. Differential contribution of monocytes to heart macrophages in steady-state and after myocardial infarction. *Circ Res.* 2014; 115:284–295. [PubMed: 24786973]
28. Chong JJ, Reinecke H, Iwata M, Torok-Storb B, Stempien-Otero A, Murry CE. Progenitor cells identified by PDGFR-alpha expression in the developing and diseased human heart. *Stem Cells Dev.* 2013; 22:1932–1943. [PubMed: 23391309]
29. Bullock TE, Wen B, Marley SB, Gordon MY. Potential of CD34 in the regulation of symmetrical and asymmetrical divisions by hematopoietic progenitor cells. *Stem Cells.* 2007; 25:844–851. [PubMed: 17185613]

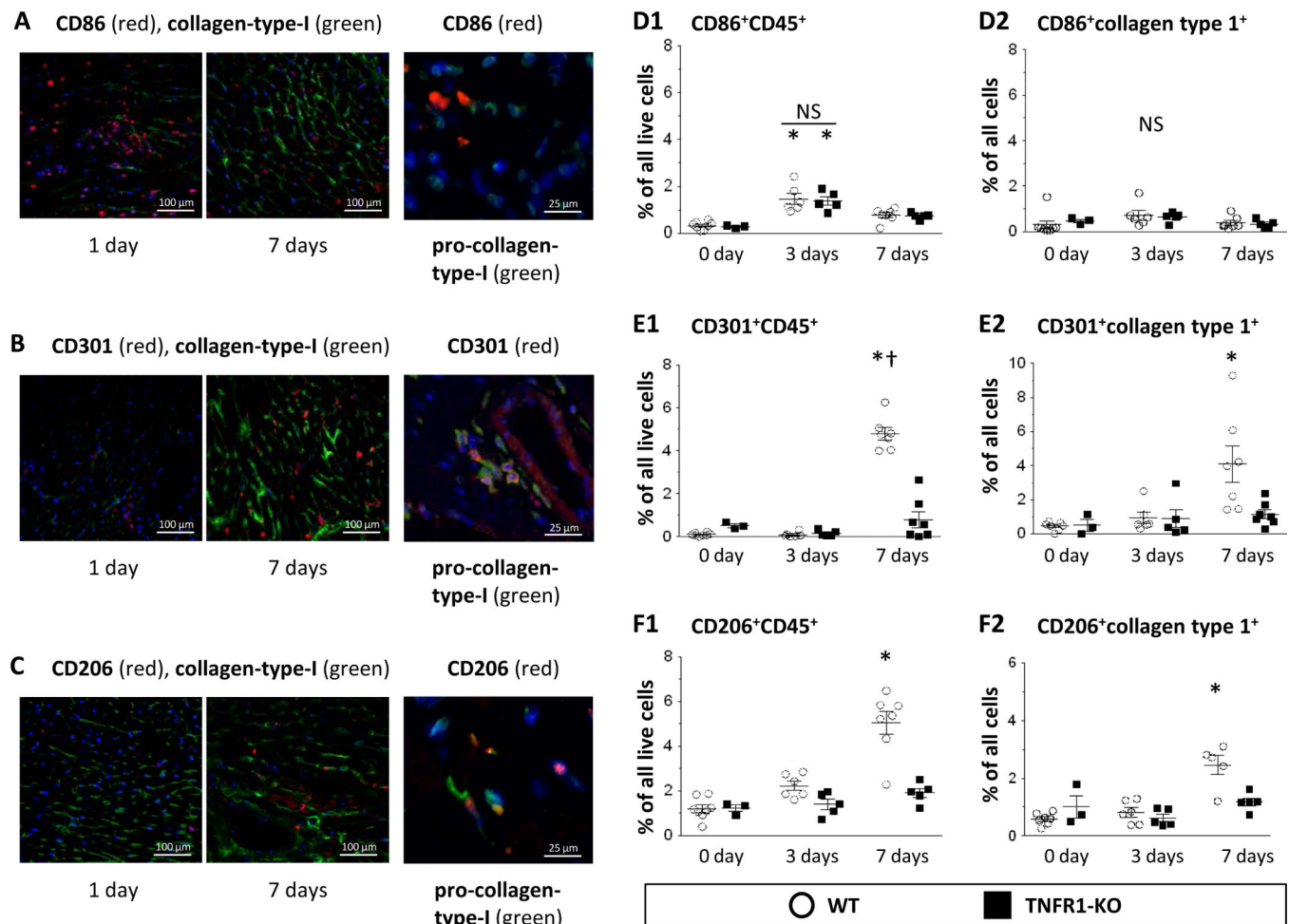


Figure 1. Temporal appearance of M1-cells and M2-cells after Ang-II infusion

A-C: Qualitative: After 1- and 7-day Ang-II infusion, WT heart sections were stained with fluorescence-labeled antibodies (blue = nuclear DAPI). Representative images are shown; they indicate an early infiltration of pro-collagen-type-I⁻ M1-cells (CD86⁺), and a later presence of pro-collagen-type-I⁺ M2-cells (CD301⁺, CD206⁺). **D-F:** Quantitative: Isolated cells from WT and TNFR1-KO hearts were subjected to cytometry. “Live” cells were identified via calcein uptake. **D1/E1/F1:** In WT hearts, hematopoietic M1-cells (CD86⁺CD45⁺) appeared maximally at 3 days, whereas M2-cells (CD301⁺CD45⁺, CD206⁺CD45⁺) increased maximally by 7 days. In TNFR1-KO mice, M1-cells were equally upregulated, but M2-cells were fewer than in WT hearts. **D2/E2/F2:** CD86⁺ cells were collagen-type-I⁻, whereas CD301⁺ and CD206⁺ cells were collagen-type-I⁺. **Statistics:** (*) indicates a statistically significant difference between saline-treated (WT: n=8; TNFR1-KO: n=3) and 3-day (WT: n=6; TNFR1-KO: n=5) or 7-day (WT: n=7; TNFR1-KO: n=5-7) Ang-II-infused mice and (†) between 3-day and 7-day Ang-II-infused mice within the same genetic background (Kruskal-Wallis, Dunn’s). NS: not significant.

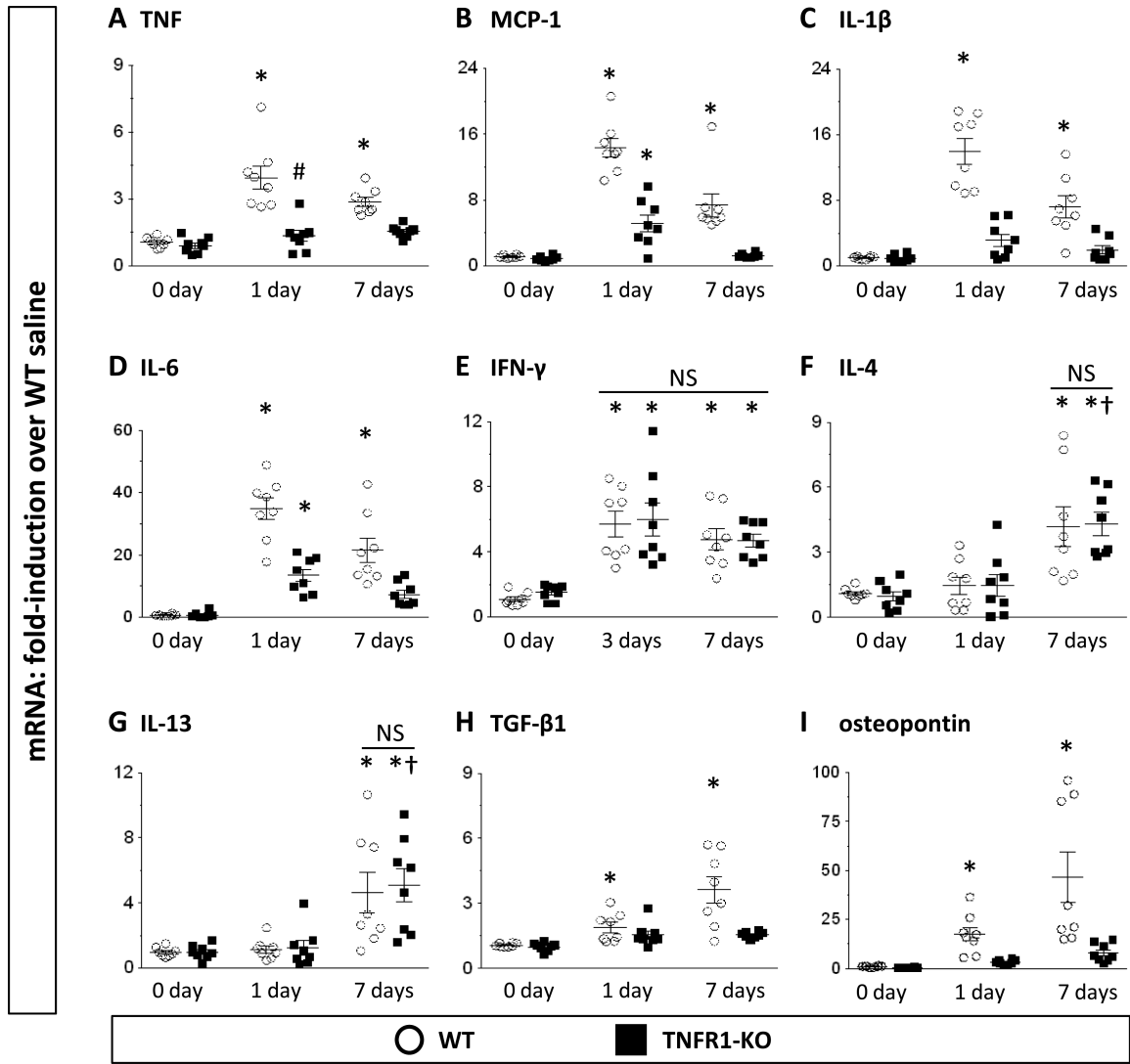


Figure 2. Transcriptional activation of inflammation- and fibrosis- related genes after Ang-II exposure

Data are represented as fold-increase over WT saline (=1-fold). Data for IFN- γ is given at 3-day Ang-II-infusion (no increase at 1-day). **Statistics:** For all groups n=8. (*) indicates a statistically significant difference between saline-treated and 1(3)-day or 7-day Ang-II-infused mice and (†) between 1-day and 7-day Ang-II-infused mice within the same genetic background; (#) between WT and TNFR1-KO groups at the same time point (Kruskal-Wallis, Dunn's). NS: not significant.

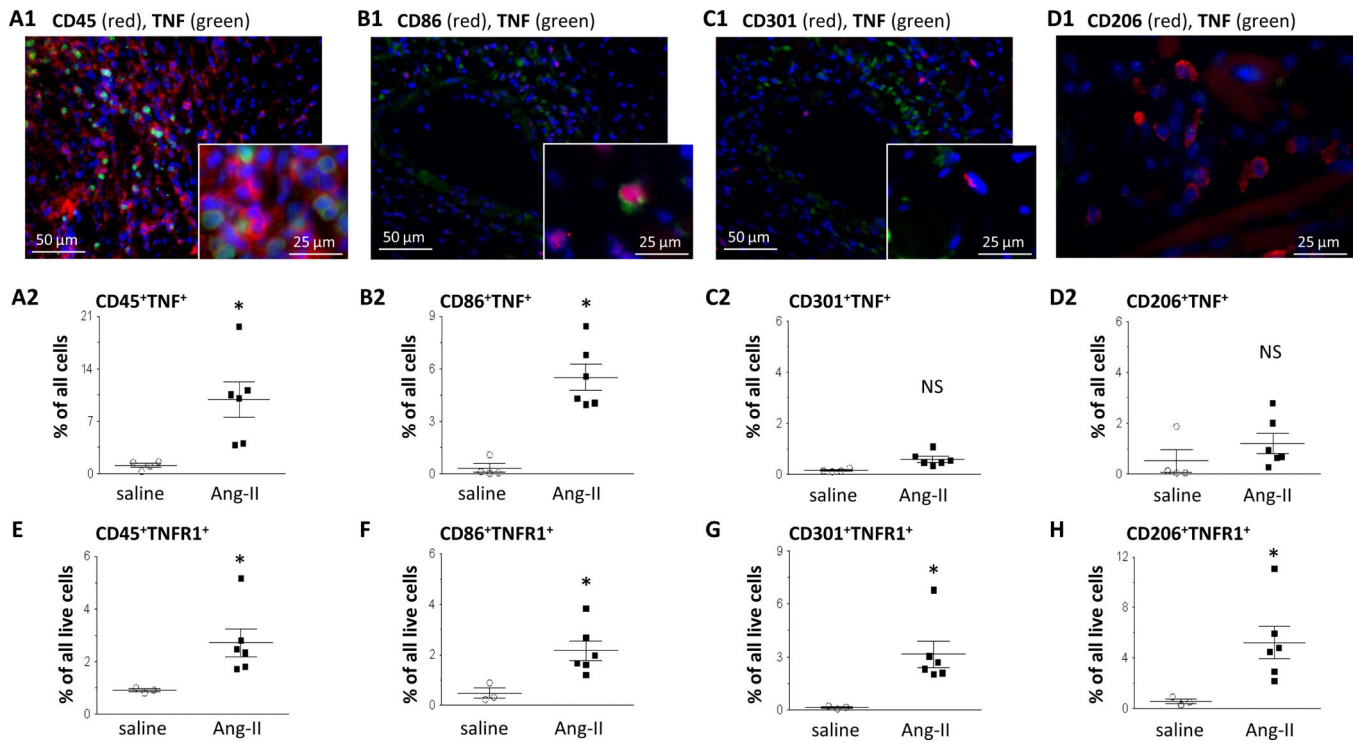


Figure 3. Cell-specific expression of TNF and TNFR1

Ang-II-treated WT hearts were either stained with fluorescence-labeled antibodies (blue = nuclear DAPI) (qualitative), or used for cytometry (quantitative). **A-D**: Representative images for TNF expression above their quantitative data, both indicating that TNF was highly expressed by CD45⁺ (A1/A2) and CD86⁺ cells (B1/B2), but not by CD301⁺ (C1/C2) or CD206⁺ (D1/D2) cells. **E-H**: TNFR1 was expressed by most cells including CD45⁺ (E1/E2), CD86⁺ (F1/F2), CD301⁺ (G1/G2), and CD206⁺ (H1/H2) cells. **Statistics**: (*) indicates a statistically significant difference between saline-treated (n=3-4) and Ang-II-treated (n=6) WT groups (two-tailed Mann-Whitney). NS: not significant.

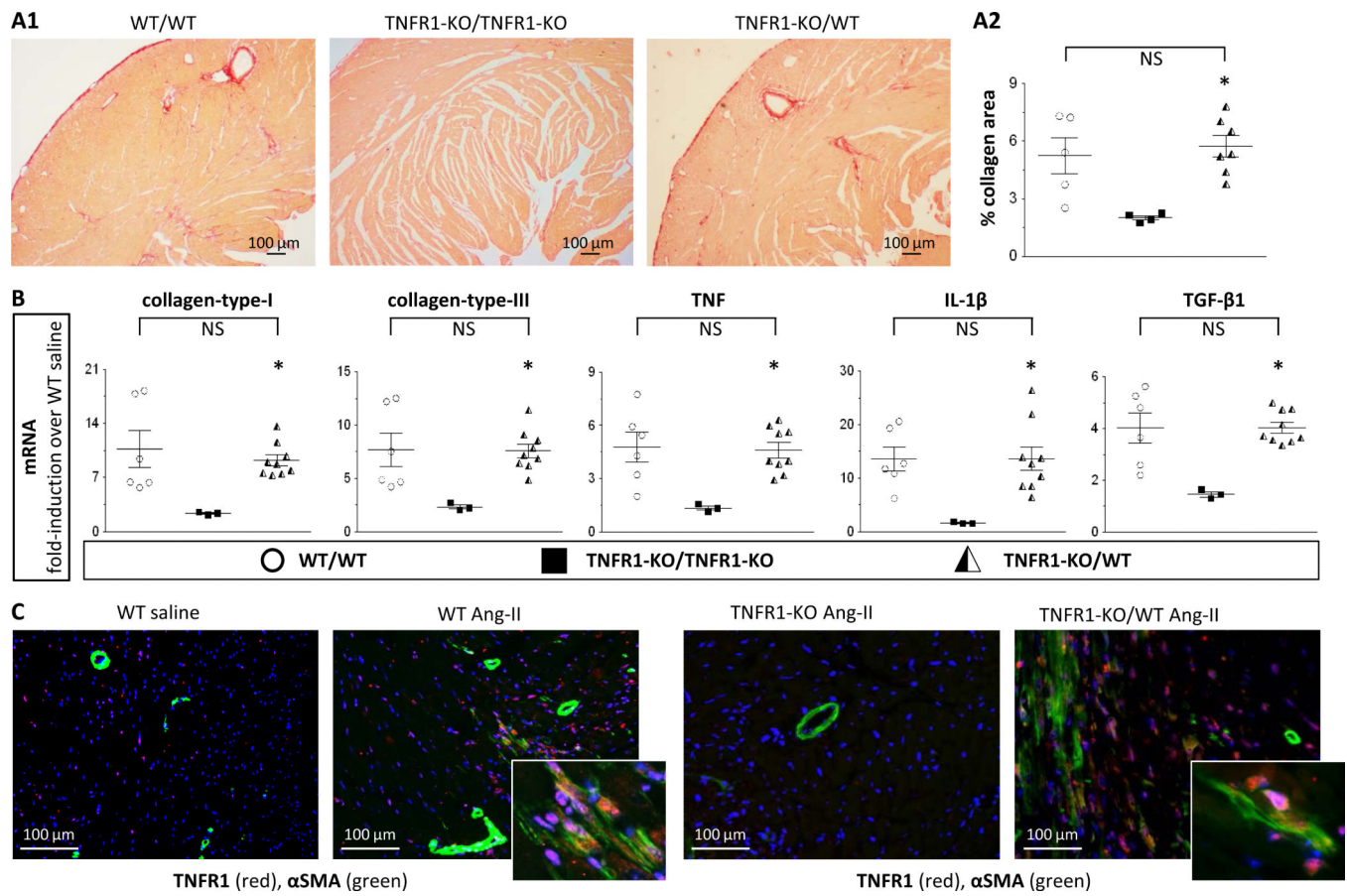


Figure 4. Lineage tracing: TNFR1 signaling in development of fibrosis

Mice (WT with WT-bone marrow [WT/WT], TNFR1-KO with TNFR1-KO-bone marrow [TNFR1-KO/TNFR1-KO], and TNFR1-KO with WT-bone marrow [TNFR1-KO/WT]) were exposed to 7-day Ang-II. **A:** Perfusion-fixed tissue was stained with picrosirius red for collagen detection; representative images (A1; Suppl.Fig.9) and quantitative analysis (A2) are shown. Chimeric TNFR1-KO/WT mice (n=7) developed interstitial cardiac fibrosis similar to WT/WT mice (n=5) and more than TNFR1-KO/TNFR1-KO mice (n=4). **B:** Transcriptional activation of selected genes. Chimeric TNFR1-KO/WT mice (n=9) showed increased mRNA levels of collagen-types -I and -III, TNF, IL-1 β , and TGF- β 1, similar to WT/WT levels (n=6) and higher than TNFR1-KO/TNFR1-KO levels (n=3). **C:** Perfusion-fixed tissue was stained for TNFR1 and α SMA; representative images are shown (blue = nuclear DAPI; quantification: Suppl.Fig.10). **Statistics:** (*) indicates a statistically significant difference between TNFR1-KO/TNFR1-KO and TNFR1-KO/WT groups (Kruskal-Wallis, Dunn's). NS: not significant.

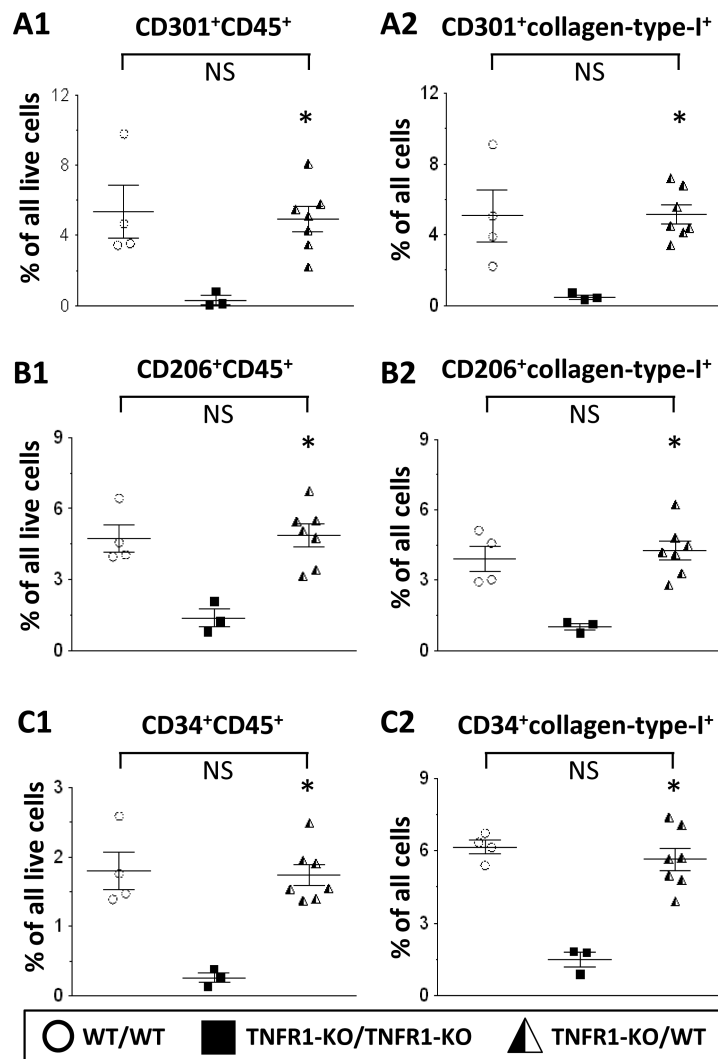


Figure 5. Lineage tracing: TNFR1 signaling in fibroblast precursor uptake

Chimeric mice (see Fig.4) were subjected to 7-day Ang-II infusion. Isolated cells were subjected to cytometry. **A1/B1/C1:** In chimeric TNFR1-KO/WT hearts, CD301⁺CD45⁺, CD206⁺CD45⁺, and CD34⁺CD45⁺ cells were increased compared to TNFR1-KO/TNFR1-KO hearts and were comparable to levels seen in WT/WT (n=3). **A2/B2/C2:** In chimeric TNFR1-KO/WT hearts, CD301⁺, CD206⁺, and CD34⁺ cells were also collagen-type-I⁺, similar to WT levels. **Statistics:** (*) indicates a statistically significant difference between TNFR1-KO/WT (n=7) and TNFR1-KO/TNFR1-KO (n=3) groups (Kruskal-Wallis, Dunn's). NS: not significant.

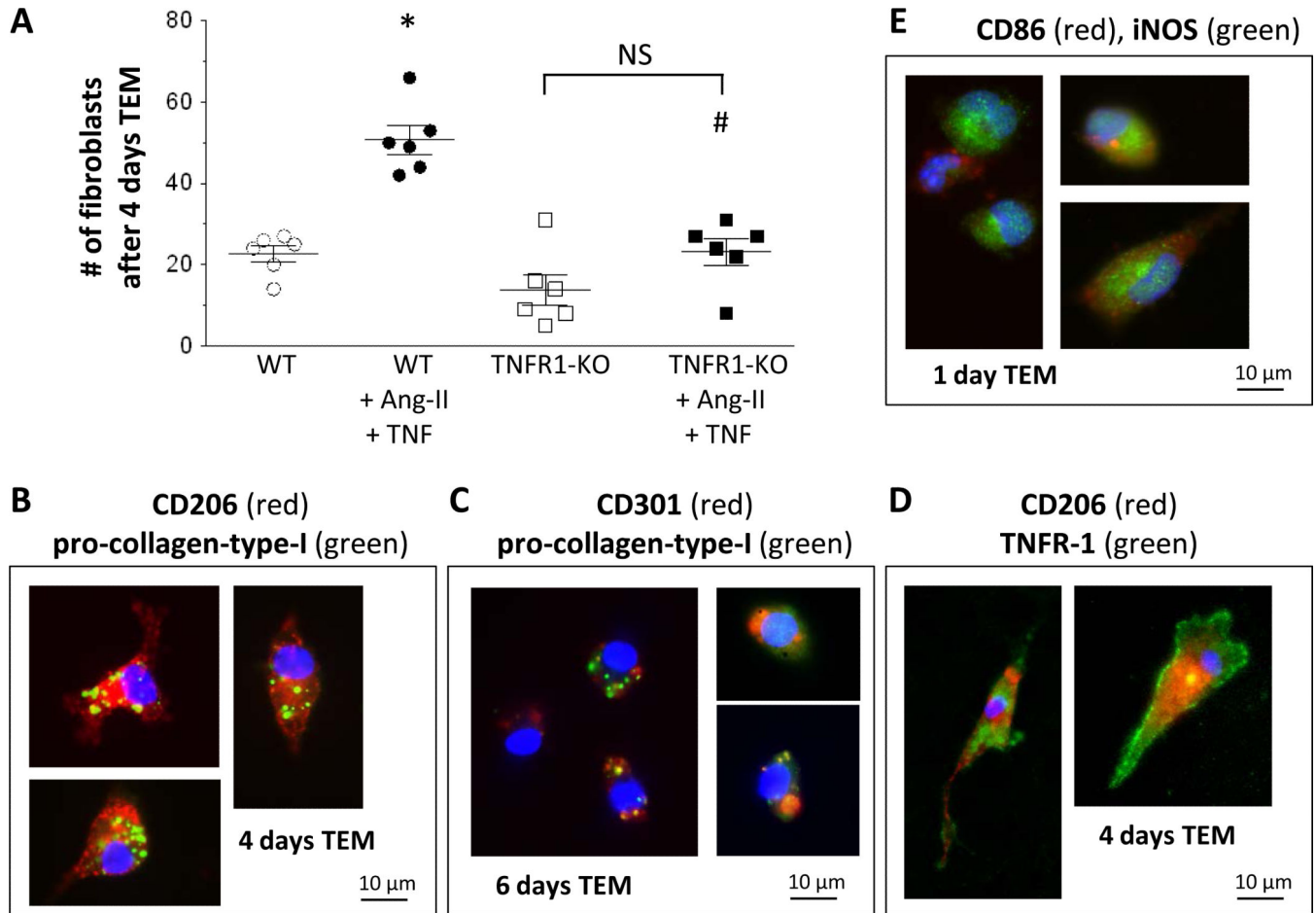


Figure 6. In vitro differentiation of mouse monocytes-to-fibroblasts

Mouse monocytes migrated through a confluent mouse endothelial layer in response to MCP-1. Successfully migrated cells were counted and characterized. **A:** Quantitative: Addition of Ang-II and TNF increased the amount of fibroblasts in WT cells, but not in TNFR1-KO. **B-E:** Qualitative: representative images of immunofluorescence staining. Cells after 4 days were spindle-shaped, CD206⁺, and pro-collagen-type-I⁺ (B); continued culturing resulted in CD301⁺pro-collagen-type-I⁺ cells (C). M2-cells (CD206⁺) also expressed TNFR1 (D). Cells after 1 day were small, round, and positive for M1 markers (CD86, iNOS; E). **Statistics:** For all groups n=6. (*) indicates a statistically significant difference between unstimulated WT and stimulated WT groups; (#) between stimulated WT and stimulated TNFR1-KO groups (one-way ANOVA, Tukey-Kramer). NS: not significant.

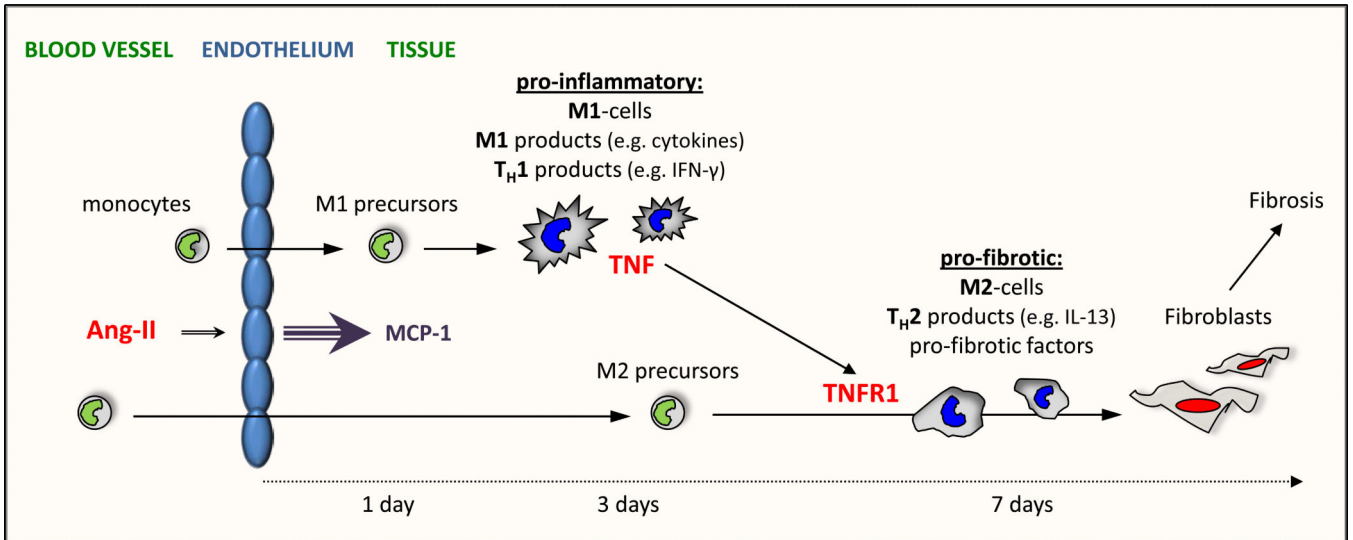


Figure 7. Hypothetical Model for the Ang-II/TNF link

Ang-II infusion results in the MCP-1-driven uptake of M1 precursors that mature to M1-cells and produced M1-related factors which, together with T_H1-related protein production, create a pro-inflammatory setting. Within a week, this setting progresses into a pro-fibrotic environment driven by the MCP-1-mediated uptake of M2 precursors and synthesis of T_H2-interleukines and pro-fibrotic factors. In this pro-fibrotic milieu some M2-cells further mature into collagen-producing fibroblasts. TNF, initially secreted by pro-inflammatory cells, aids this transition via TNFR1 signaling on distinct M2-cells that is necessary for their differentiation into fibroblasts.